Protein Cell 2010, 1(8): 771–779
DOI 10.1007/s13238-010-0085-z

Protein & Cell

RESEARCH ARTICLE

Structural basis for prokaryotic calcium-mediated regulation by a *Streptomyces coelicolor* calcium binding protein

Xiaoyan Zhao[1*], Hai Pang[1*], Shenglan Wang[2], Weihong Zhou[3], Keqian Yang[2] ✉, Mark Bartlam[3] ✉

[1] Laboratory of Structural Biology, Tsinghua University, Beijing 100084, China
[2] Center for Microbial Metabolism and Metabolic Engineering, Institute of Microbiology, Chinese Academy of Sciences, Beijing 100101, China
[3] Tianjin Key Laboratory of Protein Science, College of Life Sciences, Nankai University, Tianjin 300071, China
✉ Correspondence: yangkq@im.ac.cn (K. Yang), bartlam@nankai.edu.cn (M. Bartlam)
Received June 7, 2010 Accepted June 10, 2010

ABSTRACT

The important and diverse regulatory roles of Ca^{2+} in eukaryotes are conveyed by the EF-hand containing calmodulin superfamily. However, the calcium-regulatory proteins in prokaryotes are still poorly understood. In this study, we report the three-dimensional structure of the calcium-binding protein from *Streptomyces coelicolor*, named CabD, which shares low sequence homology with other known helix-loop-helix EF-hand proteins. The CabD structure should provide insights into the biological role of the prokaryotic calcium-binding proteins. The unusual structural features of CabD compared with prokaryotic EF-hand proteins and eukaryotic sarcoplasmic calcium-binding proteins, including the bending conformation of the first C-terminal α-helix, unpaired ligand-binding EF-hands and the lack of the extreme C-terminal loop region, suggest it may have a distinct and significant function in calcium-mediated bacterial physiological processes, and provide a structural basis for potential calcium-mediated regulatory roles in prokaryotes.

KEYWORDS calcium-binding protein, crystal structure, *Streptomyces coelicolor*, calcium-mediated regulation, EF-hand

INTRODUCTION

The important and diverse regulatory roles of Ca^{2+} in eukaryotic cells are mediated by the Ca^{2+}-sensor proteins of the calmodulin superfamily (Strynadka and James, 1989; Clapham, 1995). These helix-loop-helix EF-hand proteins (Babu et al., 1988) convey the Ca^{2+} signal through ion-induced conformational changes, followed by functional changes for the recognition of target molecules (Ikura et al., 1992). The proteins of the calmodulin superfamily can also interact with metal ions for buffering or transporting roles in eukaryotes, where the functions of both Ca^{2+}-buffer and sensor proteins have been well studied (Ikura, 1996).

In contrast, the Ca^{2+}-sensor roles of prokaryotic calcium-binding proteins are still hypothetical or poorly understood, despite repeated reports of the presence of bacterial calcium binding proteins with functional EF-hand motifs (Onek and Smith, 1992; Norris et al., 1996), and accumulated evidence that Ca^{2+} ions are involved in a myriad of physiologically important bacterial activities, including sporulation, virulence, septation, chemotaxis and phosphorylation (Norris et al., 1991; Michiels et al., 2002). The first prokaryotic calcium binding protein discovered to contain four canonical helix-loop-helix EF-hand motifs was calerythrin, a 20-kDa acidic protein from the high G + C Gram-positive bacterium *Saccaropolyspora erythraea* (Leadlay et al., 1984; Swan et al., 1987), which is proposed to function as a Ca^{2+} buffer rather than as a Ca^{2+} sensor (Cox and Bairoch, 1988).

*These authors contributed equally to the work.

The structural study of an 18 kDa calcium binding protein from the model actinomycete *Streptomyces coelicolor* A3(2) (GenBank ID: CAC08420), named CabD, should provide insights into its potential calcium-mediated role in prokaryotes, since there is evidence that overexpression of CabD in the filamentous, soil-dwelling, Gram-positive bacteria Genus *Streptomyces* essentially affects the aerial mycelium formation (unpublished data), which has been established to be calcium-dependent and calcium-mediated in actinomycetes (Natsume et al., 1989; Natsume and Marumo, 1992). The low sequence similarity (less than 28%) between CabD and other prokaryotic EF-hand proteins (Swan et al., 1987; Bylsma et al., 1992; Xi et al., 2000; Yang, 2001; Yonekawa et al., 2001; Michiels et al., 2002; Tossavainen et al., 2003), suggests that it has a distinctive and significant functions in physiologic processes in bacteria.

CabD is a compact globular protein with a pair of helix-loop-helix EF-hand motifs forming the N- and C-terminal domains of the molecule, and a predominantly hydrophobic core comprising about 20 aromatic residues. CabD is understood to share significantly high structural similarity with eukaryotic sarcoplasmic calcium binding proteins (SCP) (Cook et al., 1991; Vijay-Kumar and Cook, 1992; Cook et al., 1993), which are presumed to function as intracellular Ca^{2+} buffers in the muscle and neurons of various invertebrates (Hermann and Cox, 1995). Although the sequence homology is lower than 22%, the highest value from NSCP, a SCP from the sandworm *Nereis diversicolor* (Vijay-Kumar and Cook, 1992). This low sequence but high structural similarity with SCPs implies that CabD shares a common Ca^{2+} buffering role with the SCPs. However, a calcium-mediated regulatory role has been ascribed to calexcitin B, a member of the neuronal SCPs (Gombos et al., 2001). The locally unique tertiary fold of calexcitin evidently reveals its regulatory role in addition to GTPase activity (Erskine et al., 2006).

Here we report the first crystal structure of the *Streptomyces coelicolor* calcium binding protein determined to 1.5 Å resolution. The three-dimensional structure of CabD reveals several remarkable differences from other typical calcium binding proteins containing functional EF-hand motifs. The rarely bending orientation of the first C-terminal helix displaces it from the base of the hydrophobic pocket, spatially providing the capability to interact with the putative target molecule. Moreover, the abundance of hydrophobic amino acid residues in the vicinity of the third calcium-binding loop and the five ligands coordinating the Ca^{2+} ion probably contribute to the lower capacity to coordinate metal ions and the local conformational plasticity. Additionally,, the lack of the extreme C-terminal loop region, which is ubiquitously present in other prokaryotic calcium binding proteins and SCPs, exposes the buried cavity and renders it more accessible for target recognition. Our work provides a structural basis for understanding the potential calcium-mediated role of prokaryotic calcium binding proteins.

RESULTS

Structural overview

Two crystal forms were obtained with good diffraction to higher than 2.0 Å resolution. The crystal structure of a selenomethionyl (Se-Met) derivative in space group $P2_12_12_1$ (cell dimensions a = 32.9, b = 51.0, c = 87.0 Å, α = 90, β = 90, γ = 90), consisting of one protein molecule and 172 water molecules in the asymmetric unit, was determined by multi-wavelength anomalous diffraction (MAD) at 1.5 Å resolution and refined to an R_{work} of 19.7 % and an R_{free} of 24.8% (Table 1). 98.7% of the residues in the final structure lie in the "most favored" regions of the Ramachandran plot by the PROCHECK criteria (Laskowski et al., 1993) and 1.3% of them within the "additionally allowed" region. Two amino acid residues, Leu37 and Ile99, were selectively mutated to methionine for preparation of a selenomethionyl derivative. A native structure was also determined from the isomorphous Se-Met structure to an R_{work} of 21.0% and an R_{free} of 24.0% (Table 1). The root mean square deviation of the superimposition of the native and Se-Met structure is only 0.23 Å, which means the two structures have identical conformations. The structure is complete from residue 5 to 169, and residues 82–85 are less well defined from the structure due to the poor electron density for a small number of residues at the N-terminal end and the flexible packing region.

A different crystal form in space group P1 (a = 36.9, b = 40.1, c = 52.2 Å, α = 90, β = 90, γ = 90) was crystallized following treatment with 10 mM of the chelating agent EGTA during purification in an attempt to remove Ca^{2+} from the native structure. The structure, however, still has Ca^{2+} bound, despite the presence of two molecules per asymmetric unit and an average r.m.s. deviation with the first crystal form of 0.9 Å, which means there were only minor conformational changes around the EF-hands (data not shown).

Overall structure of CabD

The three-dimensional structure of CabD confirms that it is a compact globular molecule with overall dimensions of approximately 35 Å × 40 Å × 45 Å. The structure includes eight α-helices (A: residues 6–17, B: 27–41, C: 48–68, D: 83–91, E: 93–111, F: 121–131, G: 135–145, H: 155–166), encompassing approximately 61% of the structure. Two neighboring α-helices and the connecting loop compose the helix-loop-helix EF-hand motif, and the first and last pairs of EF-hands associate closely to form the N-terminal (residues 1–91) and C-terminal (residues 93–170) domains of the molecule by the interhelical connection (Fig. 1A). EF-hand pairs separated on opposite sides of the molecule are linked by a bend consisting of only one residue, Lys92, and are arranged so as to form a pronounced hydrophobic core comprising of about 20 aromatic residues. An electrostatic

Table 1 Data collection and refinement statistics for the native and selenomethionyl CalD from *Streptomyces coelicolor*

data collection statistics		
	native	Se-Met
space group	$P2_12_12_1$	$P2_12_12_1$
unit-cell parameters (Å)	*a* = 32.9, *b* = 51.0, *c* = 87.0	*a* = 33.1, *b* = 51.1, *c* = 87.3
resolution range (Å)	50–1.80 (1.91–1.80)	50–1.50 (1.55–1.50)
total reflections	91,632	161,520
unique reflections	21,409 (1,683)	23,403 (2,212)
R_{merge}[a] (%)	5.4 (33.7)	7.4 (39.6)
completeness (%)	98.9 (94.6)	95.4 (92.4)
average I/σ (I)	11.9 (2.8)	12.5 (2.5)
mean redundancy	4.3 (3.5)	6.9 (6.6)
refinement statistics		
R_{work} (%)	19.7	21.0
R_{free} (%)	24.8	24.0
No. of non-hydrogen atoms		
protein atoms	1224	1250
solvent	209	204
r.m.s. deviation from ideal values		
bond length (Å)	0.014	0.012
bond angle (deg.)	1.34	1.46
average B-factor (Å^2)		
protein atoms	18.3	14.2
solvent molecules	22.9	18.2

Values for the outer resolution shell of each dataset are shown in parentheses.

[a] $R_{merge}=\Sigma_h\Sigma_i\left|(I_{hi}-I_h)\right|/\Sigma_h\Sigma_i(I_{hi})$, where I_h is the mean intensity of the scaled observations I_{hi}.

Data between 50.0 Å and 1.8 Å resolution were used with no σ (F) cutoff.

surface representation of the molecule demonstrates that CabD has a hydrophobic cavity formed by the N-terminal helix A and the C-terminal helices G, H at its top, while the electrostatic surface of the terminal calcium binding sites exhibit predominately negative potential, which confer the accessibility of cation binding within these regions (Fig. 2).

Unlike other helix-loop-helix calcium binding proteins with known structure (Babu et al., 1988; Satyshur et al., 1988; Vijay-Kumar and Cook, 1992; Cook et al., 1993; Tossavainen et al., 2003), all of the non-helical portions of the EF-hand motifs do not contain short antiparallel β-sheets, but instead adopt loop segments. Nevertheless, main chain hydrogen bonds do occur between residues Ile25 and Ile76, which occupy the eighth position of each N-terminal calcium binding loop. Main chain hydrogen bonds also occur between Val119 and Val153 in the equivalent position in the C-terminal EF-hand domain (Fig. 1B and 1C).

Although there are apparent similarities between the two EF-hand domains of the CabD structure, comparing the interhelical angles and the individual calcium-binding loops indicate considerable differences between them (Table 2). The C-terminal half generally appears to be more compact than the N-terminal, owing mainly to the smaller angle between helices A/B of the first EF-hand motif and the near antiparallel arrangement of helices B and C from the two adjacent EF-hands in N-terminal side.

Table 2 Interhelical angles (°) in related four-domain calcium-binding proteins

helix pair	CabD	Nereis SCP[a]	calerythrin[b]
A/B	69	67	78
B/C	152	167	151
C/D	97	80	101
E/F	110	110	107
F/G	129	123	127
G/H	118	100	113

[a] Nereis SCP, 2SCP.pdb.

[b] Calerythrin, 1NYA.pdb.

Interhelical angles were calculated using INTERHLX (K.Yap, University of Toronto, Canada).

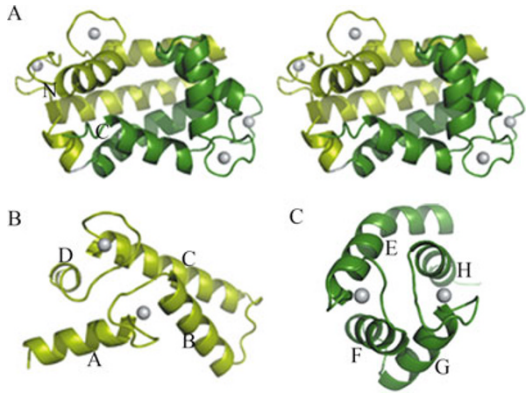

Figure 1. The tertiary structure of the calcium binding protein CabD from *Streptomyces coliecolor*. All four EF-hands are involved in binding calcium ions (shown in gray). (A) A stereo view of the domain structure of CabD with the N-terminal domain shown in light green and the C-terminal domain colored dark green. The N- and C-terminal ends of the protein are indicated, and the α-helices are labeled from A to H. (B) The N-terminal domain (resides 5–91) viewed along the pseudo 2-fold axis. (C) The C-terminal end (residues 93–169) viewed along the same axis but from the opposite direction.

Calcium binding sites

All four EF-hands are involved in binding metal ions, and the central sequence of the EF-hands possesses the typical feature of a 12-residue functional loop, where the first nine residues are from the loop region and the last three from the beginning of the next helix (Table 3). For a typical 12-residue calcium binding loop, there are usually seven ligands to each metal ion: six from relatively conserved residues, and one from a solvent molecule (Strynadka and James, 1989). The calcium binding residues at positions 1, 3, 5 are highly conserved, and the most C-terminal residue coordinating the metal ion with both carboxyl oxygen atoms is usually a conserved acidic glutamate residue. The main-chain oxygen of the seventh residue is also involved in metal ion binding, but the sequence at this position is varied. In CabD, however, several changes to the calcium-coordinating residues contribute to certain notable differences between the two halves, as well as a distinctive feature of the C-terminal EF-hand pair.

Although the two N-terminal calcium binding sites are similar to the typical ones, the first calcium binding loop (residues 18–29) adopts a more compact geometry due to a substitution of the conserved glutamate residue at position 12 in most authentic EF-hands for aspartate (Fig. 3A). The

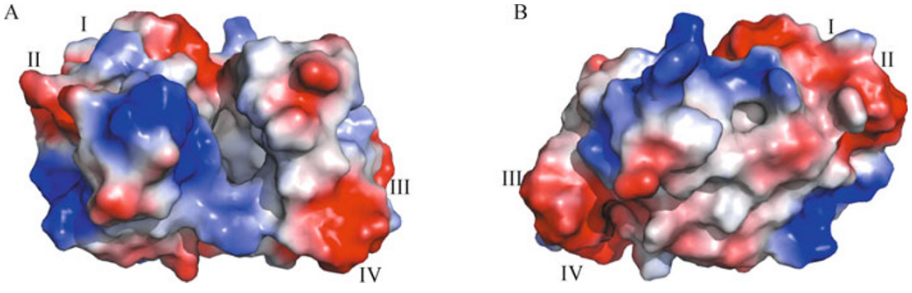

Figure 2. The electrostatic surface potential of *Streptomyces coelicolor* calcium binding protein CabD. (A) The molecule oriented as in Fig. 1A demonstrates that CabD has a pronounced hydrophobic cavity (indicated by green arrow) with helix A from the N-terminal domain and helices G, H from the C-terminal domain at its top. The electrostatic surface of the terminal calcium-binding sites exhibits predominately negative potential. (B) The molecule viewed from the opposite direction around the vertical axis. The binding loops are noted from I to IV, and the positive and negative potential are conventionally coded in blue and red, respectively.

Table 3 Residues forming the four EF-hand motifs of CabD

EF-hand	I	II	III	IV
residues forming the helices	6–17, 27–41	48–68, 78–91	93–111, 121–131	135–145, 155–166
metal ligands	Asp18 OD1	Asp69 OD1	Asp112 OD1	Asp146 OD1
	Asp20 OD1	Asp71 OD1	Asp114 OD1	Asp148 OD1
	Asn22 OD1	Asp73 OD1	Asp116 OD1	Asp150 OD1
	His24 O	Arg75 O	Ala118 O	Lys152 O
	Asp29 OD1	Glu80 OE1	W3	Glu157 OE1
	Asp29 OD2	Glu80 OE2		Glu157 OE2
	W1	W2		

The coordinating solvent molecule is indicated by W.
Ca^{2+}-O bond lengths is approximately 2.2–2.7 Å.

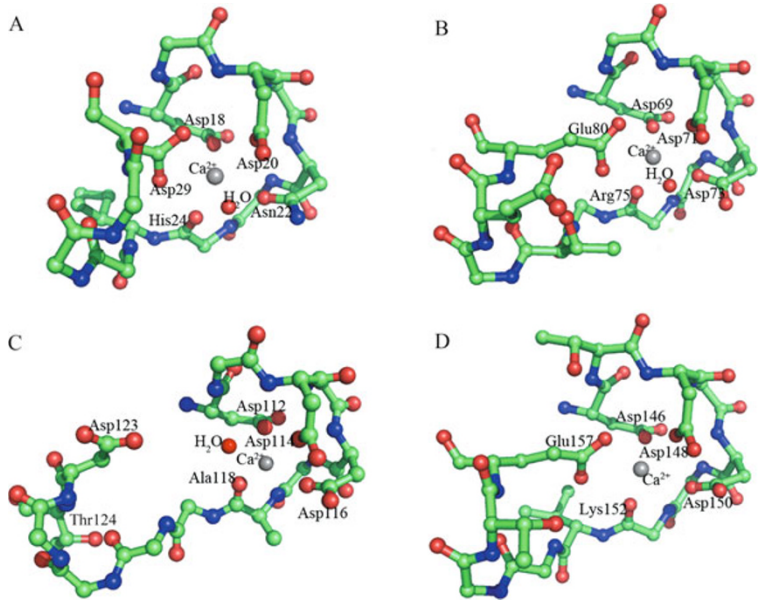

Figure 3. The four calcium binding sites in *Streptomyces coelicolor* calcium binding protein CabD. (A) The first calcium-binding site (residues 18–29) much resembles the typical one, providing seven ligands to the metal ion, six from the relatively conserved residues and one from a solvent molecule in spite of adopting a more compact geometry. (B) The metal ligands of the second site (residues 69–80) also have the typical feature of a 12-residue calcium binding loop, and the overall conformational arrangement is similar to the first. (C) The third calcium binding site (residues 112–123) lack of two Ca^{2+}-O hydrogen bonds to the Ca^{2+} binding, which is probably ascribed to the involvement of the neighboring residue Thr124 in the forming of the hydrophobic core and thus the displacement of the two carboxyl oxygen of residue Asp123 apart from the cation binding region located among the environment of the hydrophilic surface. (D) For EF-hand IV (residues 146–157), there are only six protein ligands to the metal ion without a solvent molecule. The remarkably unpaired ligand-coordinating EF-hands in the C-terminal region renders this domain markedly less symmetrical than the N-terminal domain.

shorter side chain of aspartate requires the interhelical angle to be smaller and changes the orientation of the second helix with respect to the first. There is one solvent ligand for each Ca^{2+} in both of the N-terminal calcium binding sites, but only the water molecule in site I is hydrogen-bonded to the ninth residue of the binding loop (Asp26). No such interaction is observed in the other EF-hands, where the equivalent residues are smaller and more neutral (Thr77, Thr120, Gly152 for EF-hands II, III and IV). The metal ligands of the second site (residues 69–80) have the typical features of a 12-residue calcium binding loop, and the overall conformational arrangement is similar to the first (Fig. 3B). The proximity of the first two calcium binding sites indicates the strong cooperative interaction of the Ca^{2+} binding within the N-terminal side.

The Ca^{2+} ligands of the third calcium-binding site (residues 112–123) in the C-terminal side are quite different from a functional Ca^{2+}-loaded EF-hand domain, although the key sequence is in accordance with the N-terminal (Strynadka and James, 1989). This site coordinates the metal ion using four protein ligands and one water molecule, while residue Asp123 at position 12, which is well defined by the electron density map, does not participate in metal ion binding. Moreover, the hydrophobic amino acid resides are quite abundant in the vicinity of this site, where the seventh residue providing the main-chain oxygen for the metal coordinating is also a hydrophobic alanine residue but not the common basic amino acids present in the other three motifs (Fig 3C). The fourth calcium binding site (residues 146–157) assumes a slightly different ligand binding form, where all of the six ligands are offered by the residues at the designated positions of the binding site without solvent molecule (Fig. 3D).

Comparison to Nereis SCP and calerythrin

Although the sequence homology between CabD and *Nereis* sarcoplasmic calcium binding protein NSCP (Vijay-Kumar and Cook, 1992) is rather low (22%), a structural comparison between CabD and the eukaryotic SCPs reveals strong similarity in their tertiary structures (Fig. 4). The structure of NSCP (PDB code: 2scp) solved at 2.0 Å resolution can be superimposed onto CabD with an r.m.s. deviation of 2.21 Å. The orientation of the two ends is slightly asymmetric: 1.97 Å and 2.26 Å for the N- and C-terminal, respectively. This moderately reflects the different conformation between the N- and C-terminal domains of the molecule.

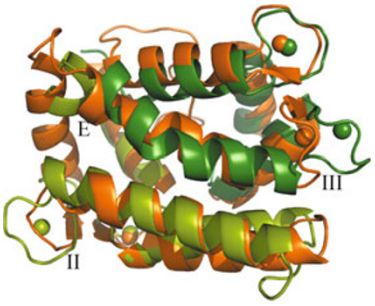

Figure 4. A superposition of CabD (shown in green) with the structure of *Nereis* sarcoplasmic calcium binding protein NSCP (shown in orange). The structures are more similar in the N-termianl domains (shown in light green for CabD) than in the C-terminal domains (shown in dark green for CabD) where there are notable conformation divergence in the positions of helix E (shown in the foreground). The markedly different orientations in the vicinity of calcium binding sites II and III are also noted.

CabD and NSCP have broadly similar interhelical angles (Table 2). The notably smaller angle between A/B helix pair was observed in both structures. SCPs have a high affinity for Ca^{2+} in the functional calcium binding EF-hands, and also possess a third high affinity site in either the second or fourth EF-hand (Cook et al., 1991).The slightly divergent angle and ~5 Å distance separating the C/D helix pair partly results from the nonfunctional Ca^{2+}-free NSCP, in contrast to the Ca^{2+} binding helix-loop-helix domain of CabD. The angles between helices B and C indicate that they are both nearly antiparallel, and the interhelical angles in the C-terminal side are nearly similar.

Other divergences in local conformation also appear in the vicinity of the kink connecting the two ends, and the orientation of the first C-terminal helix, which primarily constitutes the base of the buried cavity. The orientation of the linking loop of CabD deviates substantially from that of NSCP: there is only one amino acid (Lys92) in the loop region of CabD, whereas the equivalent region in SCPs is usually a tight 4-residue linker between helices D and E. Nonetheless, the backbone in both proteins changes direction so as to bring the two ends closely together. The C-terminal halves of both proteins also exhibit significant differences, owing mainly to the unique orientation of helix E in CabD and the longer C-terminal loop of NSCP. The two markedly separate helical regions of helix E (residues 93–99 and 103–111) in CabD result from a bend in the middle due to the presence of a proline residue (Pro102), whereas the conformation of all helices in NSCP are straight and form the environment of the buried core. The long C-terminal loop beyond the last EF-hand, consisting of 15 amino acid residues in NSCP, can be observed in the interface between the N- and C-terminal halves where it packs between helices A, B and H. The lack of an equivalent long C-terminal loop containing only four residues (167–170) in CabD enables the buried cavity to be more accessible to putative ligands.

Overall, the tertiary conformation of CabD is essentially similar to the structures of SCPs, which are assumed to have a Ca^{2+}-buffering role, and the most divergent part between the proteins is located in the extreme C-terminal loop region (Fig. 5). Several presumably four-domain EF-hand proteins have been identified in *Streptomyces coelicolor* (Bentley et al., 2002). It is interesting to note that most of the eukaryotic Ca^{2+}-buffering proteins and prokaryotic calcium-binding proteins (Michiels et al., 2002), such as the widely-studied four-domain calcium-binding protein calerythrin from *Saccharopolyspora erythraea*, all contain a long C-terminal loop consisting of a number of highly conserved amino acid residues, which is shown to tuck back among the α-helices forming the top of the hydrophobic pocket (Fig. 6).

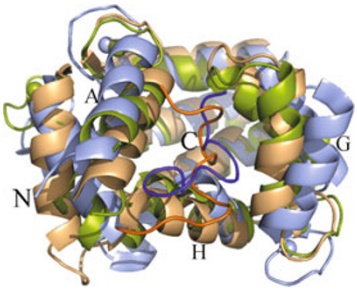

Figure 5. A superposition of CabD (shown in green) with the structure of calerythrin (shown in light magenta) and NSCP (shown in light orange), both containing a longer C-terminal loop region. The extreme C-terminal loop beyond the last EF-hand of NSCP (brown) and calerythrin (violet) appears to tuck back into the top of the hydrophobic cavity where helices A, G and H encompass, which has been implicated in most of other Ca^{2+}-buffering proteins. The lack of this loop region of CabD makes the opening of hydrophobic pocket more accessible to the putative target binding.

DISCUSSION

Implications for the biological role of CabD

The biological role of calcium binding proteins is strongly related to the metal binding affinity and the structural response to ion binding (Rabah et al., 2005). The high affinity calcium binding site assumes a Ca^{2+}-regulatory role and is conformationally less sensitive to ion loading. In contrast, the lower affinity site is likely to play a Ca^{2+}-buffering role and undergo significant ion-induced conformational changes. The three-dimensional structure of the *Streptomyces coelicolor* calcium binding protein CabD reveals some unique conformational features and thus the distinctive potential role of the protein mediated by Ca^{2+}.

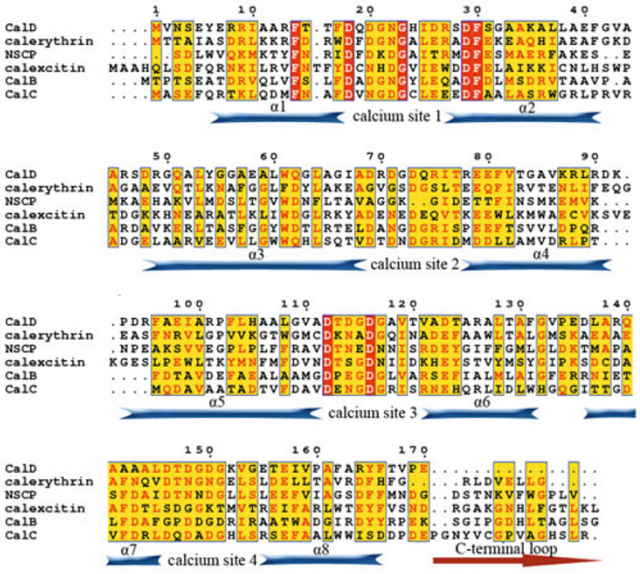

Figure 6. A sequence alignment of *Streptomyces coelicolor* calcium binding proteins CabD with other related EF-hand proteins. CabD shares 28%, 22% and 26% sequence identity with the other related protein sequences from the well-studied *Saccharopolyspora erythraea* calcium binding protein calerythrin, *Nereis* sarcoplasmic calcium binding protein NSCP, and the *Loligo pealei* neuronal calcium-sensor protein calexcitin. The sequence of the other calcium binding proteins from *Streptomyces coelicolor* indicated as CalB and CalC are also shown. The identical residues are highlighted in red, while similar residues are shown in yellow. The secondary structure elements and calcium binding sites of the *Streptomyces coelicolor* calcium binding protein CabD are indicated below the alignment. It is notable that CabD lacks the extreme C-terminal loop region highlighted with red, which is ubiquitously present in other prokaryotic calcium binding proteins and sarcoplasmic calcium binding proteins.

A range of physical studies have shown that pairs of helix-loop-helix motifs retain their structure and affinity to Ca^{2+} binding. The pair of N-terminal calcium binding domains that appear to be fully occupied by calcium ions coordinated by seven ligands may fulfill a Ca^{2+}-regulatory role with high affinity for Ca^{2+}. However, the two C-terminal calcium binding sites provide markedly unpaired metal ligands, with five and six ligands, respectively, and are proposed to have weaker affinity for calcium ions. As a consequence, they may exert a more rapid response for Ca^{2+} binding and release and could be described as having a Ca^{2+}-buffering role. Furthermore, the third calcium binding site possesses a number of unusual features, including an abundance of hydrophobic residues in the vicinity of this site and a lack of two Ca^{2+}-O hydrogen bonds to the Ca^{2+} ion, which is probably due to the involvement of the neighboring residue Thr124 in formation of the hydrophobic interior, and thus the displacement of the two carboxyl oxygens of residue Asp123 from the cation binding region located among the environment of the hydrophilic surface. The tertiary structure shows that the hydrophobic side-chains in the vicinity of the third calcium binding site most likely tend to interact with the hydrophobic surroundings as they cannot be well matched by positively charged groups and presumably hold some conformational plasticity among this site of the molecule.

The specific bending orientation of helix E displaces its middle portion away from the base of the hydrophobic pocket and provides more capability for the putative target recognition, which is moderately demonstrated by the pair of long stretches of electron density present in the hydrophobic cavity. We have so far been unable to identify the corresponding ligand and these stretches of electron density remain unmodeled in the final structure. From the annotation of the diverse roles of Ca^{2+} in bacterial physiologic processes, the binding ligands might be some universal biosynthetic products derived from some Ca^{2+}-modulated activities binding as cellular targets via hydrophobic interaction.

The lack of an extreme C-terminal loop beyond EF-hand IV of CabD, which is present in most other Ca^{2+}-buffering proteins and which shares a strongly conserved sequence, makes the opening of the hydrophobic pocket more accessible for putative target recognition or binding. Although repeated reports have shown that many prokaryotic proteins possess four canonical calcium-binding EF-hand motifs, their Ca^{2+}-mediated regulatory role is still hypothetical or poorly understood (Michiels et al., 2002). Our study of the three-dimensional structure of the calcium binding protein CabD provides a structural basis for the Ca^{2+}-mediated biologic role in prokaryotes. Further structural and functional studies will inevitably reveal if a ubiquitous Ca^{2+} regulator, analagous to

calmodulin in eukaryotes, is present in prokaryotes and the role of helix-loop-helix EF-hands in prokaryotic cellular processes mediated by calcium ions.

MATERIALS AND METHODS

Protein expression and purification

The plasmid pET-44B-CabD originally used to express the CabD protein was subcloned into the bacterial expression vector pGEX-6p-1 (GE Healthcare) using *Bam*HI and *Eco*RI restriction sites. The recombinant plasmid was transformed into *Escherichia coli* strain BL21 (DE3) and over-expressed as a glutathione-S-transferase (GST) fusion protein. Cells were harvested, and resuspended in 1 × phosphate-buffer saline (10 mM sodium phosphate pH 7.4, 150 mM NaCl) and lysed by sonication. The lysate was centrifuged at 27,000 *g* at 277 K for 30 min and the cell debris was discarded. The supernatant was loaded onto a GST-glutathione column (Qiagen) and cleaved with 200 μg of GST-rhinovirus 3C protease. The target protein was washed down and further applied to a Resource Q anion-exchange chromatography column and a Superdex-75 size-exclusion column (Pharmacia). The purified and concentrated protein (10 mg/mL) was stored in 20 mM HEPES (pH 7.5) at 193 K. Two site-directed mutations, L37M and I99M, were introduced by PCR for preparation of a selenomethionyl derivative protein. L-SetMet-labeled protein was purified and stored under the same conditions as the native protein.

Crystallization

The crystallization of CabD has been reported elsewhere (Zhao et al., 2008). Briefly, CabD protein solution used for crystallization contained 20 mM HEPES (pH 7.5) and 10 mg/mL protein. Crystals optimized for X-ray diffraction were obtained using the hanging drop vapor diffusion technique with reservoir solution containing 12%–16% (*v/v*) PEG8000, 0.1 M cacodylate sodium (pH 6.5), 0.2 M zinc chloride. Protein solution (1.5 μL) was mixed with reservoir solution (1.5 μL) and equilibrated against 200 μL of reservoir solution at 291K. The Se-Met derivative crystal was grown from the same conditions.

Data collection and processing

A single CabD crystal was harvested using a nylon loop (Hampton Research) and flash-cooled to 100 K in a nitrogen stream prior to data collection. Multi-wavelength anomalous diffraction (MAD) data for L-SetMet-labeled CabD protein were collected using radiation of wavelengths 0.9788, 0.9793, and 0.9700 Å on a MAR CCD detector on beamline 3W1A of the Beijing Synchrotron Radiation Facility. Data were processed and scaled using the HKL2000 package (Otwinowski and Minor, 1997) (Table 1).

Structure determination, refinement and analysis

The CabD structure was solved by the MAD technique using L-SetMet-labeled protein. The anomalous diffraction data were sufficient to solve the phase problem and yielded clear experimental electron density maps. Two selenium positions were determined, and initial phases were calculated by the program SOLVE (Terwilliger and Berendzen, 1999). Following density modification by RESOLVE (Terwilliger, 2000), the resulting electron density map was of sufficient quality that the entire model, with the exception of several residues at the N- and C-termini, could be built. The program Coot (Emsley and Cowtan, 2004) was used for manual rebuilding of the model, and further refinements were performed using Refmac5 (Murshudov et al., 1997) in the CCP4 suite (1994). Sequence alignment was performed using ClustalW (Thompson et al., 1994). Comparison of three-dimensional structures was carried out using the DALI server (Holm and Sander, 1998).

PROTEIN DATA BANK ACCESSION CODES

The coordinates and structure factors have been deposited with the RCSB Protein Data Bank and assigned the accession numbers 3AKA and 3AKB for the native and Se-Met structures, respectively.

ACKNOWLEDGEMENTS

This project was supported by the National Natural Science Foundation of China (Grant Nos. 30400259, 30221003), the National Basic Research Program (973 Program) (Grant No. 2007CB914301), and the Tianjin Municipal Science and Technology Commission (Grant No. 08SYSYTC00200).

REFERENCES

Babu, Y.S., Bugg, C.E., and Cook, W.J. (1988). Structure of calmodulin refined at 2.2 A resolution. J Mol Biol 204, 191–204.

Bentley, S.D., Chater, K.F., Cerdeño-Tárraga, A.M., Challis, G.L., Thomson, N.R., James, K.D., Harris, D.E., Quail, M.A., Kieser, H., Harper, D., *et al*. (2002). Complete genome sequence of the model actinomycete Streptomyces coelicolor A3(2). Nature 417, 141–147.

Bylsma, N., Drakenberg, T., Andersson, I., Leadlay, P.F., and Forsén, S. (1992). Prokaryotic calcium-binding protein of the calmodulin superfamily. Calcium binding to a Saccharopolyspora erythraea 20 kDa protein. FEBS Lett 299, 44–47.

Clapham, D.E. (1995). Calcium signaling. Cell 80, 259–268.

Collaborative Computational Project, Number 4. (1994). The CCP4 suite: programs for protein crystallography. Acta Crystallogr D Biol Crystallogr 50, 760–763.

Cook, W.J., Ealick, S.E., Babu, Y.S., Cox, J.A., and Vijay-Kumar, S. (1991). Three-dimensional structure of a sarcoplasmic calcium-binding protein from Nereis diversicolor. J Biol Chem 266, 652–656.

Cook, W.J., Jeffrey, L.C., Cox, J.A., and Vijay-Kumar, S. (1993). Structure of a sarcoplasmic calcium-binding protein from amphioxus refined at 2.4 A resolution. J Mol Biol 229, 461–471.

Cox, J.A., and Bairoch, A. (1988). Sequence similarities in calcium-binding proteins. Nature 331, 491.

Emsley, P., and Cowtan, K. (2004). Coot: model-building tools for molecular graphics. Acta Crystallogr D Biol Crystallogr 60, 2126–2132.

Erskine, P.T., Beaven, G.D., Hagan, R., Findlow, I.S., Werner, J.M., Wood, S.P., Vernon, J., Giese, K.P., Fox, G., and Cooper, J.B. (2006). Structure of the neuronal protein calexcitin suggests a mode of interaction in signalling pathways of learning and memory. J Mol Biol 357, 1536–1547.

Gombos, Z., Jeromin, A., Mal, T.K., Chakrabartty, A., and Ikura, M. (2001). Calexcitin B is a new member of the sarcoplasmic calcium-binding protein family. J Biol Chem 276, 22529–22536.

Hermann, A., and Cox, J.A. (1995). Sarcoplasmic calcium-binding protein. Comp Biochem Physiol B Biochem Mol Biol 111, 337–345.

Holm, L., and Sander, C. (1998). Touring protein fold space with Dali/FSSP. Nucleic Acids Res 26, 316–319.

Ikura, M. (1996). Calcium binding and conformational response in EF-hand proteins. Trends Biochem Sci 21, 14–17.

Ikura, M., Clore, G.M., Gronenborn, A.M., Zhu, G., Klee, C.B., and Bax, A. (1992). Solution structure of a calmodulin-target peptide complex by multidimensional NMR. Science 256, 632–638.

Laskowski, R.A., Moss, D.S., and Thornton, J.M. (1993). Main-chain bond lengths and bond angles in protein structures. J Mol Biol 231, 1049–1067.

Leadlay, P.F., Roberts, G., and Walker, J.E. (1984). Isolation of a novel calcium-binding protein from Streptomyces erythreus. FEBS Lett 178, 157–160.

Michiels, J., Xi, C., Verhaert, J., and Vanderleyden, J. (2002). The functions of Ca(2+) in bacteria: a role for EF-hand proteins? Trends Microbiol 10, 87–93.

Murshudov, G.N., Vagin, A.A., and Dodson, E.J. (1997). Refinement of macromolecular structures by the maximum-likelihood method. Acta Crystallogr D Biol Crystallogr 53, 240–255.

Natsume, M., and Marumo, S. (1992). Calcium signal modulators inhibit aerial mycelium formation in Streptomyces alboniger. J Antibiot (Tokyo) 45, 1026–1028.

Natsume, M., Yasui, K., and Marumo, S. (1989). Calcium ion regulates aerial mycelium formation in actinomycetes. J Antibiot (Tokyo) 42, 440–447.

Norris, V., Chen, M., Goldberg, M., Voskuil, J., McGurk, G., and Holland, I.B. (1991). Calcium in bacteria: a solution to which problem? Mol Microbiol 5, 775–778.

Norris, V., Grant, S., Freestone, P., Canvin, J., Sheikh, F.N., Toth, I., Trinei, M., Modha, K., and Norman, R.I. (1996). Calcium signalling in bacteria. J Bacteriol 178, 3677–3682.

Onek, L.A., and Smith, R.J. (1992). Calmodulin and calcium mediated regulation in prokaryotes. J Gen Microbiol 138, 1039–1049.

Otwinowski, Z., and Minor, W. (1997). Processing of X-ray diffraction data collected in oscillation mode. In Macromolecular Crystallography, part A, C.W. Carter Jr., and R.M. Sweet, eds. (Academic Press), pp. 307–326.

Rabah, G., Popescu, R., Cox, J.A., Engelborghs, Y., and Craescu, C. T. (2005). Solution structure and internal dynamics of NSCP, a compact calcium-binding protein. FEBS J 272, 2022–2036.

Satyshur, K.A., Rao, S.T., Pyzalska, D., Drendel, W., Greaser, M., and Sundaralingam, M. (1988). Refined structure of chicken skeletal muscle troponin C in the two-calcium state at 2-A resolution. J Biol Chem 263, 1628–1647.

Strynadka, N.C., and James, M.N. (1989). Crystal structures of the helix-loop-helix calcium-binding proteins. Annu Rev Biochem 58, 951–999.

Swan, D.G., Hale, R.S., Dhillon, N., and Leadlay, P.F. (1987). A bacterial calcium-binding protein homologous to calmodulin. Nature 329, 84–85.

Terwilliger, T.C. (2000). Maximum-likelihood density modification. Acta Crystallogr D Biol Crystallogr 56, 965–972.

Terwilliger, T.C., and Berendzen, J. (1999). Automated MAD and MIR structure solution. Acta Crystallogr D Biol Crystallogr 55, 849–861.

Thompson, J.D., Higgins, D.G., and Gibson, T.J. (1994). CLUSTAL W: improving the sensitivity of progressive multiple sequence alignment through sequence weighting, position-specific gap penalties and weight matrix choice. Nucleic Acids Res 22, 4673–4680.

Tossavainen, H., Permi, P., Annila, A., Kilpeläinen, I., and Drakenberg, T. (2003). NMR solution structure of calerythrin, an EF-hand calcium-binding protein from Saccharopolyspora erythraea. Eur J Biochem 270, 2505–2512.

Vijay-Kumar, S., and Cook, W.J. (1992). Structure of a sarcoplasmic calcium-binding protein from Nereis diversicolor refined at 2.0 A resolution. J Mol Biol 224, 413–426.

Xi, C., Schoeters, E., Vanderleyden, J., and Michiels, J. (2000). Symbiosis-specific expression of Rhizobium etli casA encoding a secreted calmodulin-related protein. Proc Natl Acad Sci U S A 97, 11114–11119.

Yang, K. (2001). Prokaryotic calmodulins: recent developments and evolutionary implications. J Mol Microbiol Biotechnol 3, 457–459.

Yonekawa, T., Ohnishi, Y., and Horinouchi, S. (2001). A calcium-binding protein with four EF-hand motifs in Streptomyces ambofaciens. Biosci Biotechnol Biochem 65, 156–160.

